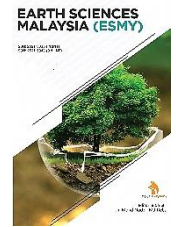


ZIBELINE INTERNATIONAL™
PUBLISHING

ISSN: 2521-5035 (Print)

ISSN: 2521-5043 (Online)

CODEN: ESMACU



RESEARCH ARTICLE

THE USE OF ACOUSTIC DOPPLER CURRENT PROFILER (ADCP) TO DETERMINE THE WATER VELOCITY AS RELATED TO SEDIMENT DEPOSITION IN EPE LAGOON, LAGOS STATE, NIGERIAIlube Oshomah Emmanuel^a, Osisanya Olajuwon Wasiu^b, Saleh Alhaji Saleh^c^a Department of Applied Geophysics, Federal University Of Technology, Akure. Ondo state.^b Department of Physics, Federal University of Petroleum Resources, Effurun, Delta State.^c Department of Petroleum Engineering and Geosciences, Petroleum Training Institute, Effurun, Nigeria*Corresponding author's email: wasiu.osisanya@uniben.edu

This is an open access journal distributed under the Creative Commons Attribution License CC BY 4.0, which permits unrestricted use, distribution, and reproduction in any medium, provided the original work is properly cited

ARTICLE DETAILS

Article History:

Received 04 December 2024

Revised 12 January 2025

Accepted 10 February 2025

Available online 25 February 2025

ABSTRACT

Sediment deposition poses significant challenges to marine transport, aquatic ecosystems, and hydrogeological exploration. This study investigates the integration of Acoustic Doppler Current Profiler (ADCP) data with grain size analysis to estimate sediment deposition velocities in a lagoonal environment. Data from ten ADCP measurements revealed varying velocities, with the highest at 7.70 ft/s and the lowest at 0.99 ft/s. Analysis of ADCP data indicated high velocity zones at depths of 21 to 27 ft and 12 to 19 ft, while low velocities were observed at shallow depths (up to 18 ft) and near the bottom at specific locations. Concurrent grain size analysis identified a predominance of coarse-grained sand, with varying degrees of sorting from moderately well to poorly sorted sediments. The results demonstrated that areas of high sediment velocity are associated with larger grain sizes, whereas low velocity zones correspond to finer grains. This study suggests optimal navigation routes for vessels around the lagoon's middle and recommends dredging edges to mitigate sediment accumulation. These insights provide valuable guidance for sediment management, coastal engineering, and marine transportation safety.

KEYWORDS

Sediment Deposition, Velocity Estimation, Grain Size Analysis, Acoustic Doppler Current profiler, Marine transport.

1. INTRODUCTION

Sediment deposition is considered extreme when it exceeds the recommended or established total maximum daily load (TMDL), which sets limits for measurable parameters in a body of water. Excessive sediment can significantly impact aquatic environments. For instance, sediment deposits in rivers and lagoons can alter water flow and reduce depth, making navigation and recreational use more difficult (Fondriest Environmental, Inc., 5 Dec. 2014). While sediment deposition can create habitats for aquatic life, excessive sediment can be detrimental. It can bury habitats, alter waterways, and disrupt natural aquatic migrations. Many spawning habitats require specific sediment sizes (e.g., gravel), and finer sediments can smother eggs and other benthic organisms. Additionally, high sediment levels can lead to poor water quality, algal blooms, and increased turbidity, which may elevate water temperatures and decrease dissolved oxygen levels (Fondriest Environmental, Inc., 5 Dec. 2014). The study of sediments and sediment transport is crucial for understanding these impacts. In recent study, authors aimed to review key concepts and techniques in modern geomorphology regarding sediments and their transport (Sherman et al., 2013). To assess sediment dynamics, instruments such as the Acoustic Doppler Current Profiler (ADCP) are employed. An ADCP measures water velocity across the entire water column, providing valuable data for understanding sediment transport. These instruments can be anchored to the seafloor or mounted on structures to measure currents in various environments (Woods Hole Oceanographic Institution, 2017).

The predecessor of the ADCP was the Doppler speed log, developed in the mid-1970s. This instrument was redesigned to measure water velocity more accurately and to allow measurements over a depth profile. Subsequent advancements in signal processing have improved the accuracy and reliability of ADCPs. A group researchers analyzed the effects of sediment inflow on the quality parameters of rivers, finding that sediments adversely affect surface water quality (Osugwu et al., 2014). The nature of sediment is influenced by geological, geomorphic, and organic factors, which determine the amount, material, and size of transported sediment. For example, rivers with mountain headwaters often carry glacial silt, while low-lying areas may collect organic material (Fondriest Environmental, Inc., 5 Dec. 2014).

Given the multifaceted impacts of sediment deposition on aquatic ecosystems, the aim of this study is to determine the rate of sediment deposition (specifically sand) in Epe Lagoon, Lagos State, Nigeria. This will be achieved through the assessment of current velocity, water current direction, sediment sample analysis, and characterization of the deposited sediment.

1.1 Descriptio Study Area

Epe lagoon is bound by coordinates (2°50'-4°10'N, 5°30' - 5°40'E) and it has a surface area of 2432 km (Kusemiju, 1988). The linear length and area covered for the data collection survey is 5.46km and 3.93km² respectively. The lagoon has an average depth of about 1.80m and situated between two other lagoon, the Lagos lagoon (brackish water) to the west and Lekki

Quick Response Code



Access this article online

Website:

www.earthsciencesmalaysia.com

DOI:

10.26480/esmy.01.2025.13.30

lagoon (freshwater) to the east. Epe lagoon is connected to the Atlantic Ocean through the Lagos lagoon (figure 1 and 2). Epe lagoon supports a major fishery in Lagos state, Nigeria and it is also used as transportation route for people, goods and timber logs from Epe to other places in south-western Nigeria. The lagoon houses the Egbin thermoelectric power plant which serves as a major source of electric power generation in Western Nigeria. The lagoon is the major source of water for the inhabitants of Epe and other villages situated along its bank. (Edokpayi and Ikharo, 2010).

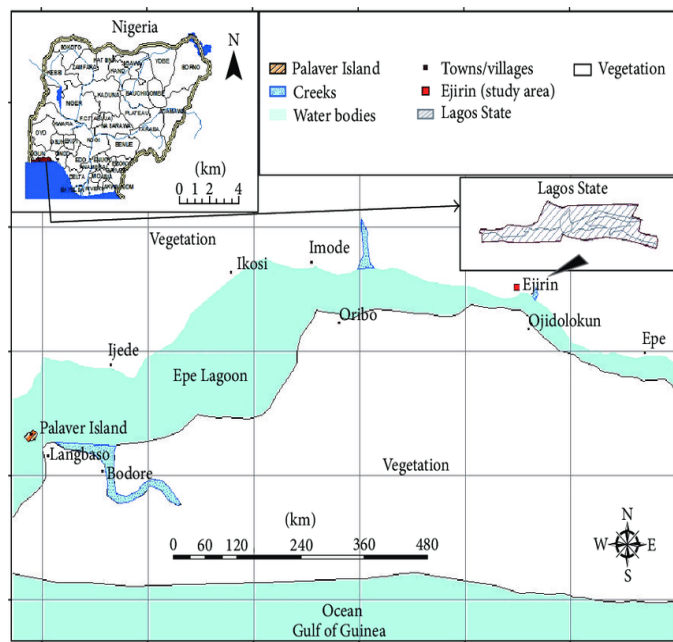


Figure 1: Base Map of the Study Area

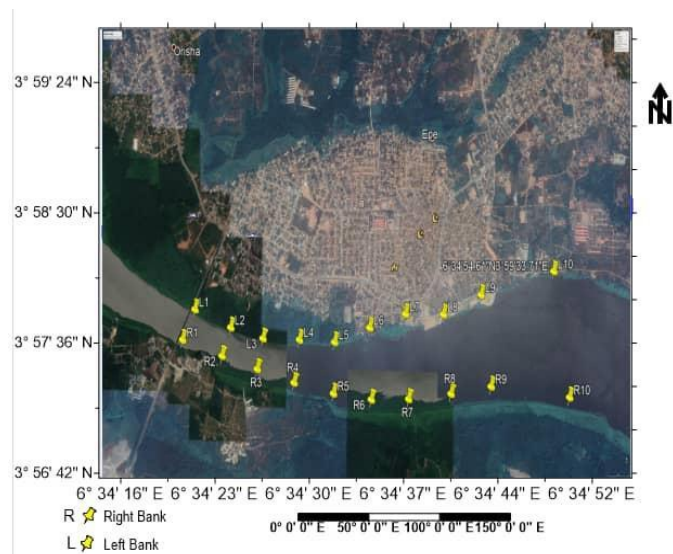


Figure 2: Map of Epe Lagoon (Researchgate, 2021).

2. MATERIALS AND METHODOLOGY

2.1 Materials

The materials utilized for the success of this research work are SxS Pro software, Microsoft Office Excel 2013, Raw ADCP data, Sediment data v. GPS data and Google Earth Pro. The raw ADCP data was given in the (.PDO) format. The total number of transect points for the acquisition of the data were 10 in the study area. The raw data contains information like: intensity of the beams, the velocity of the equipment, the direction of the velocity, and the velocity at different depths. The sediment acquired at the study site were analyzed in the laboratory and the values were saved in the excel worksheet to undergo further processing which involve the sediment size calculations using the formulas for mean, graphic standard deviation, graphic skewness and kurtosis. The values are calculated and the plotted on a log-log graph sheet. The results are then compared to the Grain Size Scales for Sediments and the calculated values are also compared to the Udden- Wentworth scale, to know their representation, see Table 1.

Table 1: Udden Wentworth Scale

Millimeters (mm)	Micrometers (µm)	Phi (φ)	Wentworth size class	
4096		-12.0	Boulder	Gravel
256		-8.0	Cobble	
64		-6.0	Pebble	
4		-2.0	Granule	
2.00		-1.0	Very coarse sand	
1.00		0.0	Coarse sand	Sand
1/2	0.50	1.0	Medium sand	
1/4	0.25	2.0	Fine sand	
1/8	0.125	3.0	Very fine sand	
1/16	0.0625	4.0	Coarse silt	Silt
1/32	0.031	5.0	Medium silt	
1/64	0.0156	6.0	Fine silt	
1/128	0.0078	7.0	Very fine silt	
1/256	0.0039	8.0	Clay	Mud
	0.00006	14.0		

2.2 GPS Data

The Garmin GPSMAP 78 was used to generate the coordinates for the location of the study area and the location from where the sediments samples were obtained. The data were in the Degree Minute Second (DMS) format.

2.3 Google Earth Pro

This is a geospatial software application that displays a virtual globe, which offers the ability to analyze and capture geographical data. Google earth was created after Google acquired CIA funded Keyhole Inc. in 2004. Under Keyhole, the application was known as Earth viewer 3D. Google earth pro offers premium high resolution photos. It helps you automatically geo-loc Geographic information system (GIS). Google earth pro offers super image overlays that are more than the main texture size. Google earth pro also lets you map multiple points at once and lets you access demographic, graphic and traffic data layers.

3. RESULTS AND DISCUSSIONS

The ADCP data acquired from ten (10) positions at the study area were processed with the Section by Section Pro software (SxS Pro), from the output of the data, the velocity was computed against depth for each sample point. Fourteen (14) sediment samples were taken from random positions around the locations where the ADCP data were taken, the results were presented as profiles on a log-log graph sheet after the results were computed on Excel software.

3.1 Acoustic Doppler Current Profiler Results

Figure 3 shows the velocity profile with a velocity of 3.5ft/s at depth 6ft to 8ft with a lesser velocity from depth 9ft to 17ft. the velocity increased from 18ft to the bottom. Figure 4 Shows a general low velocity at the signal point with the lowest velocity close to the surface at depth 5.5ft to 7ft and an increased velocity as it moves downwards but there was a drop in the velocity at depth 16ft to 18ft with a higher velocity below that depth to the bottom. Figure 5 shows a general low velocity at location 3 with the highest velocity being 2.87ft/s with the lowest velocity at 2.42ft/s. The lowest velocity at depth 8ft to 13ft is sandwiched between corresponding higher velocities above and beneath it, with the highest velocity at depth 15.5ft to 18ft and a lesser velocity beneath that to the bottom.

Figure 6 shows a general low velocity at location 4 with the highest velocity being 2.76ft/s with the lowest velocity at 1.59ft/s. The velocity increases uniformly downwards to the bottom. Figure 7 is characterized by a very low velocity with the highest being 1.67ft/s and the lowest being 1.32ft/s. The highest velocity can be seen from 5.5ft which is close to the surface to 12ft and it reduces progressively to the bottom. Figure 8 shows a general high velocity with the highest being 5.85ft/s and the lowest being 3.28ft/s. The velocity increases downwards till it got to depth 15.5ft to 18ft which was the region of the highest velocity then the velocity dropped till it got to the bottom.

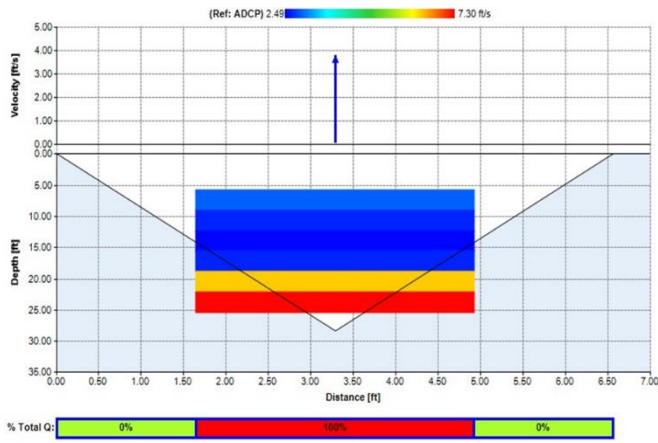


Figure 3: Water Velocity Data for Location 1

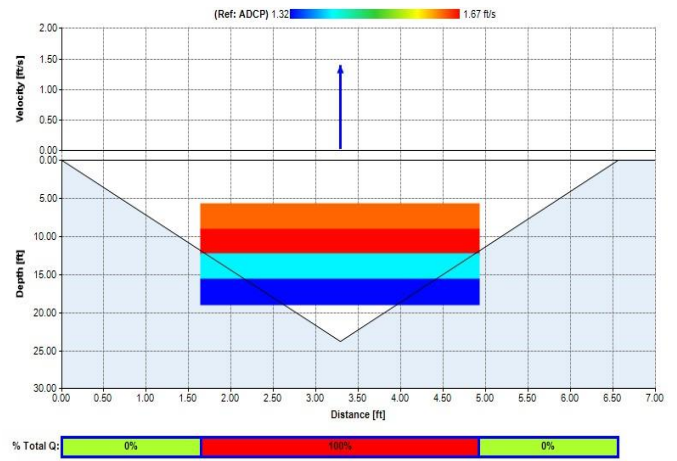


Figure 7: Water Velocity Data for Location 5

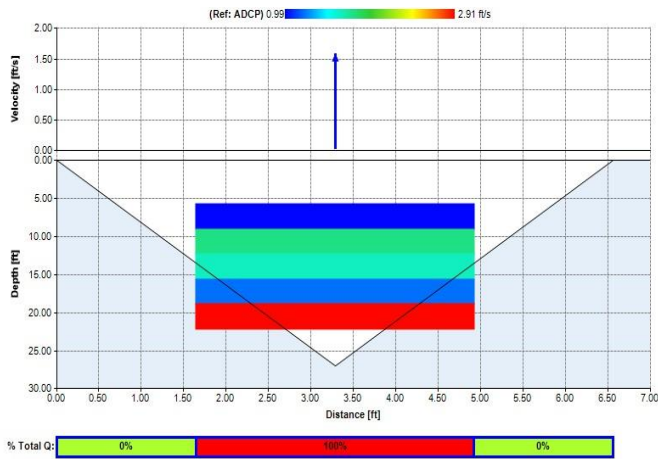


Figure 4: Water Velocity Data for Location 2

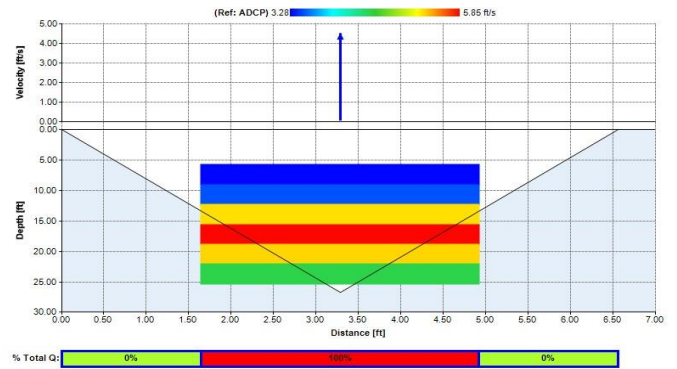


Figure 8: Water Velocity Data for Location 6

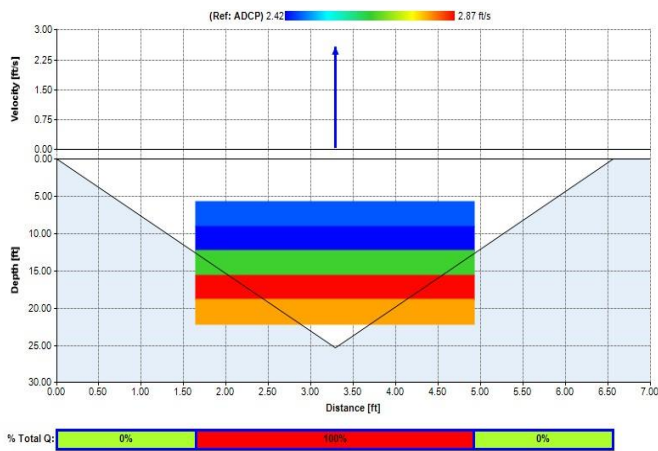


Figure 5: Water Velocity Data for Location 3

Figure 9 is characterized by a high velocity with the highest being 5.22ft/s and the lowest being 3.71ft/s. The velocity increases downwards till it got to the bottom. Figure 10 is characterized by very high velocity with the highest being 7.70ft/s and the lowest being 4.21ft/s. The velocity increases from the top till it got to the bottom. Figure 11 shows a very low velocity across generally with the highest velocity being 2.83ft/s and the lowest velocity being 2.38ft/s. The velocity increases from 5.5ft till it got to 18ft where it has it highest velocity, then there was a decrease in velocity downward till it got to the bottom. Figure 12 shows a high velocity with the highest velocity being 5.98ft/s and the lowest being 4.70ft/s. The velocity increases downwards till it got to the bottom, with the highest velocity at the bottom region.

3.2 Acoustic Dopple Current Profiler Velocity Contour Map

Figure 13 shows a velocity contour map in the study area. The top center, bottom left and the center part of the study area are characterized with low velocity as can be seen with the dark blue to moderately dark blue coloration. At depth 5ft to depth 20ft and from 27ft to 30ft in location 2 to location 9 are areas with predominant low velocities. At depth 14ft to 19ft in location 5-10 and also at depth 21ft to 28ft in location 1 to 10 is characterized with high velocity as can be seen from the light blue to white coloration.

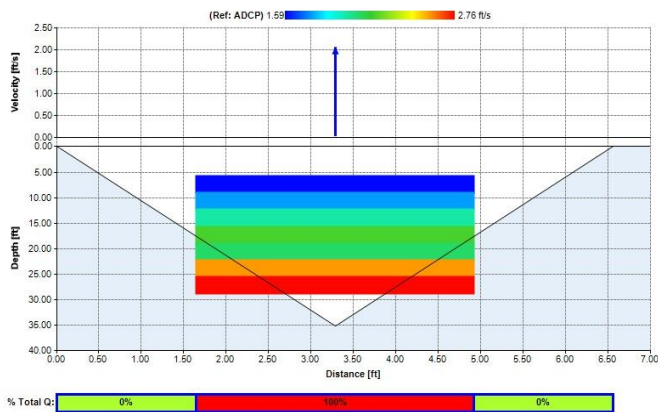


Figure 6: Water Velocity Data for Location 4

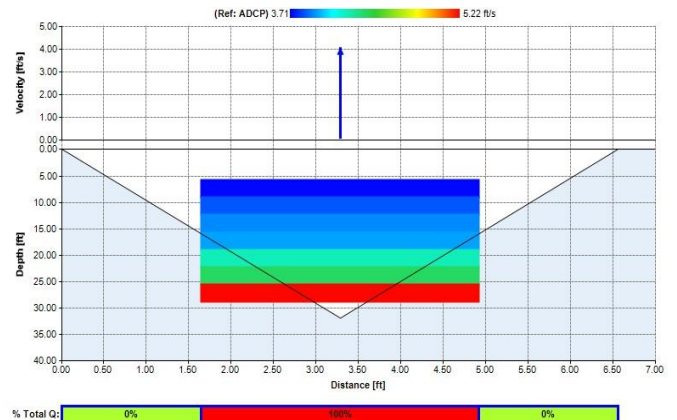


Figure 9: Water Velocity Data for Location 7

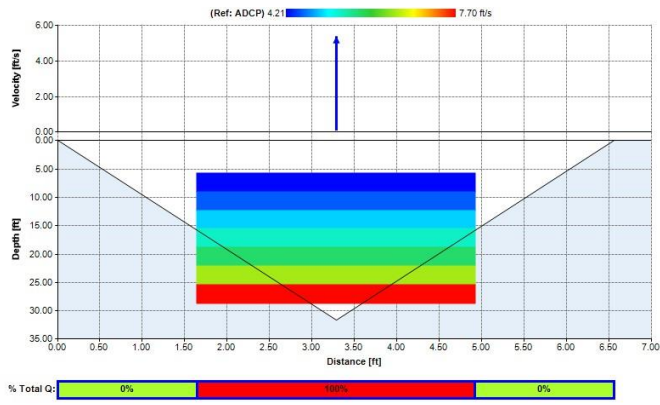


Figure 10: Water Velocity Data for Location 8.

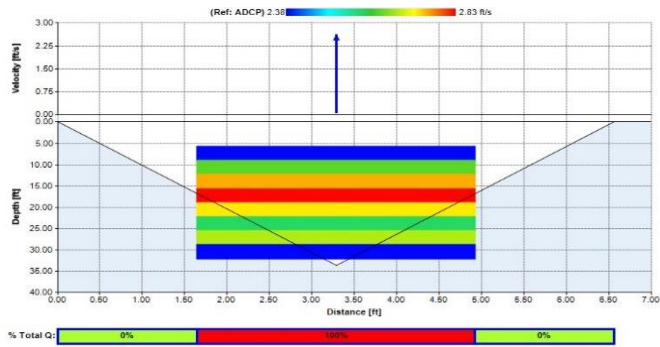


Figure 11: Water Velocity Data for Location 9

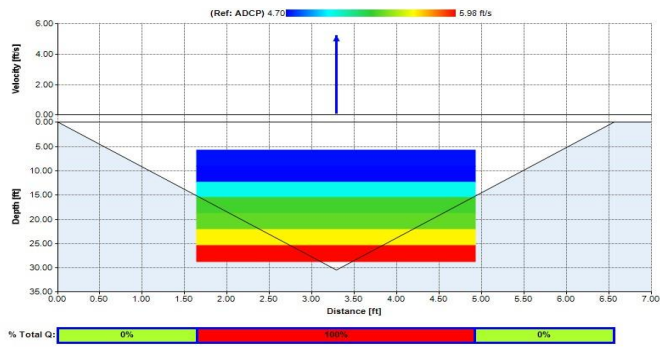


Figure 12: Water Velocity Data for Location 10

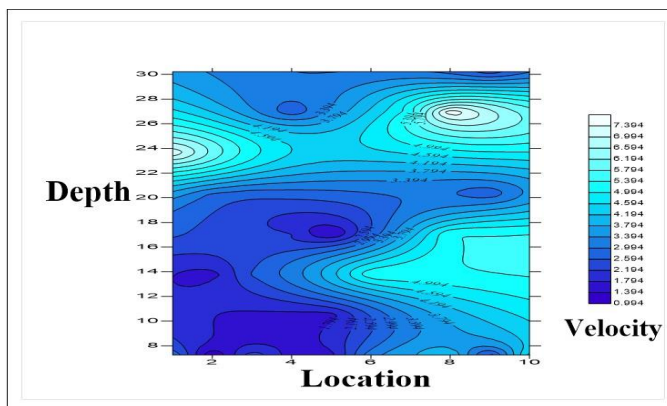


Figure 13: Water Velocity Contour Map

3.3 Grain Size Analysis Results

From Figure 15 the mean, graphic standard deviation, graphic skewness and kurtosis were calculated from the graph and the results were compared on the grain size scales for sediments (which is a data correlation sheet) in figure 14 and Table 16. From the values, the Mean value correspond to coarse sand, the Incl. graphic std. dev. value correspond to moderately sorted, the Incl. graphic skewness correspond to strongly fine skewed and the Kurtosis correspond to very Platykurtic,

Table 2. From Figure 16 the Mean value correspond to medium sand, the

Incl. graphic std dev. value correspond to very well sorted, the Incl. graphic skewness correspond to strongly fine skewed and the Kurtosis correspond to very Platykurtic, Table 3. From Figure 17 the Mean value correspond to coarse sand, the Incl. graphic std dev. value correspond to poorly sorted, the Incl. graphic skewness correspond to strongly coarse skewed and the Kurtosis correspond to very Platykurtic, Table 4. From Figure 18 the Mean value correspond to coarse sand, the Incl. graphic std dev. value correspond to moderately sorted, the Incl. graphic skewness correspond to strongly fine skewed and the Kurtosis correspond to Platykurtic. Table 5. From Figure 19 the Mean value correspond to coarse sand, the Incl. graphic std dev. value correspond to poorly sorted, the Incl. graphic skewness correspond to strongly coarse skewed and the Kurtosis correspond to Platykurtic. Table 6. From Figure 20. the Mean value correspond to coarse sand, the Incl. graphic std dev. value correspond to very well sorted, the Incl. graphic skewness correspond to strongly coarse skewed and the Kurtosis correspond to very Platykurtic. Table 7. From Figure 21 the Mean value correspond to medium sand, the Incl. graphic std dev. value correspond to very well sorted, the Incl. graphic skewness correspond to strongly coarse skewed and the Kurtosis correspond to Platykurtic. Table 8. From Figure 22 the Mean value correspond to medium sand, the Incl. graphic std dev. value correspond to moderately well sorted, the Incl. graphic skewness correspond to strongly coarse skewed and the Kurtosis correspond to Mesokurtic. Table 9

From Figure 23 the Mean value correspond to medium sand, the Incl. graphic std dev. value correspond to poorly sorted, the Incl. graphic skewness correspond to coarse skewed and the Kurtosis correspond to Mesokurtic. From Figure 24 the Mean value correspond to fine sand, the Incl. graphic std dev. value correspond to moderately sorted, the Incl. graphic skewness correspond to strongly coarse skewed and the Kurtosis correspond to Leptokurtic. Table 11. From Figure 25 the Mean value correspond to fine sand, the Incl. graphic std dev. value correspond to moderately well sorted, the Incl. graphic skewness correspond to strongly coarse skewed and the Kurtosis correspond to Leptokurtic. Table 12. From Figure 26 the Mean value correspond to coarse sand, the Incl. graphic std dev. value correspond to moderately sorted, the Incl. graphic skewness correspond to coarse skewed and the Kurtosis correspond to Platykurtic/Mesokurtic. Table 13. From Figure 27 the Mean value correspond to coarse sand, the Incl. graphic std dev. value correspond to poorly sorted, the Incl. graphic skewness correspond to coarse skewed and the Kurtosis correspond to very Platykurtic. Table 14. From Figure 28 the Mean value correspond to fine sand, the Incl. graphic std dev. value correspond to poorly sorted, the Incl. graphic skewness correspond to fine skewed and the Kurtosis correspond to very Platykurtic. Table 15.

Table 2: Station 1 Data Table						
Station 1						
Mm	µm	Ø	Freq.	Cum Freq.	CF%	Indiv. Pot.
2	2000	-1	9.06	9.06	14.37069	14.37069
1.4	1400	-0.5	5.89	14.95	23.71322	9.34253311
1	1000	0	7.495	22.445	35.60155	11.8883337
0.71	710	0.5	8.72	31.165	49.43294	13.8313903
0.5	500	1	9.03	40.195	63.75605	14.3231025
0.35	350	1.5	8.69	48.885	77.53985	13.7838052
0.25	250	2	7.515	56.4	89.45991	11.9200571
0.18	180	2.5	4.66	61.06	96.85146	7.39154572
0.125	125	3	1.575	62.635	99.34967	2.49821556
0.09	90	3.5	0.41	63.045	100	0.65032913

Mean= (Ø16+Ø50+Ø84)/ 3= 0.48 (COARSE SAND)

Incl. GRAPHIC Std. DEV. $\sigma = ((Ø84-Ø16)/4 + (Ø95-Ø5)/6.6) = 0.99$ (MODERATELY SORTED)

INCL. GRAPHIC SKEWNESS SKI = $((Ø16+Ø84-2Ø50)/2(Ø84-Ø16)) + ((Ø5+Ø95 -2Ø50)/2(Ø95-Ø5)) = 0.28$

(STRONGLY FINE SKEWED)

KURTOSIS- KG= $(Ø95-Ø5)/2.44(Ø75-Ø25) = 0.55$ (VERY PLATYKURTIC)

Table 3: Station 2 Data Table

Station 2						
Mm	µm	Ø	Freq.	Cum Freq.	CF%	Indiv. Pot.
2	2000	-1	0.335	0.335	0.531366	14.37069
1.4	1400	-0.5	0.51	0.845	1.340312	0.80894599
1	1000	0	0.84	1.685	2.672694	1.33238163
0.71	710	0.5	0.93	2.615	4.147831	1.47513681
0.5	500	1	1.27	3.885	6.162265	2.01443413
0.35	350	1.5	2.5	6.385	10.12769	3.96542152
0.25	250	2	4.97	11.355	18.01094	7.88325799
0.18	180	2.5	9.4	20.755	32.92093	14.9099849
0.125	125	3	13.07	33.825	53.65215	20.7312237
0.09	90	3.5	11.33	45.155	71.62344	17.9712903

Mean= $(\phi_{16}+\phi_{50}+\phi_{84})/3= 1.6$ (MEDIUM SAND)

Incl. GRAPHIC Std. DEV. O I = $(\phi_{84}-\phi_{16})/4 + (\phi_{95}-\phi_{5})/6.6= 0.52$ (VERY WELL SORTED)

INCL. GRAPHIC SKEWNESS SKI = $((\phi_{16}+\phi_{84}-2\phi_{50})/2(\phi_{84}-\phi_{16})) + ((\phi_{5}+\phi_{95}-2\phi_{50})/2(\phi_{95}-\phi_{5}))= 10.2$

KURTOSIS- KG= $(\phi_{95}-\phi_{5})/2.44(\phi_{75}-\phi_{25})= 0.34$ (VERY PLATYKURTIC)

Table 4: Station 3 Data Table

Station 3						
Mm	µm	Ø	Freq.	Cum Freq.	CF%	Indiv. Pot.
2	2000	-1	6.385	6.385	10.12769	14.37069
1.4	1400	-0.5	6.09	12.475	19.78745	9.65976683
1	1000	0	8.11	20.585	32.65128	12.8638274
0.71	710	0.5	8.9	29.485	46.76818	14.1169006
0.5	500	1	6.92	36.405	57.74447	10.9762868
0.35	350	1.5	5.13	41.535	65.88151	8.13704497
0.25	250	2	5.455	46.99	74.53406	8.65254977
0.18	180	2.5	7.065	54.055	85.74034	11.2062812
0.125	125	3	6.555	60.61	96.13768	10.3973352
0.09	90	3.5	4.1	64.71	102.641	6.5032913

mean= $(\phi_{16}+\phi_{50}+\phi_{84})/3= 0.7$ (COARSE SAND)

Incl. GRAPHIC Std. DEV. O I = $(\phi_{84}-\phi_{16})/4 + (\phi_{95}-\phi_{5})/6.6= 1.15$ (POORLY SORTED)

INCL. GRAPHIC SKEWNESS SKI = $((\phi_{16}+\phi_{84}-2\phi_{50})/2(\phi_{84}-\phi_{16})) + ((\phi_{5}+\phi_{95}-2\phi_{50})/2(\phi_{95}-\phi_{5}))= 2.3$

KURTOSIS- KG= $(\phi_{95}-\phi_{5})/2.44(\phi_{75}-\phi_{25})= 0.54$ (VERY PLATYKURTIC)

Table 5: Station 4 Data Table

Station 4						
Mm	µm	Ø	Freq.	Cum Freq.	CF%	Indiv. Pot.
2	2000	-1	14.065	14.065	22.30946	14.37069
1.4	1400	-0.5	10.13	24.195	38.37735	16.067888
1	1000	0	10.79	34.985	55.49211	17.1147593
0.71	710	0.5	9.63	44.615	70.76691	15.2748037
0.5	500	1	6.37	50.985	80.87081	10.103894
0.35	350	1.5	3.985	54.97	87.19169	6.32088191
0.25	250	2	2.62	57.59	91.34745	4.15576176
0.18	180	2.5	1.71	59.3	94.0598	2.71234832
0.125	125	3	0.965	60.265	95.59045	1.53065271
0.09	90	3.5	0.4	60.665	96.22492	0.63446744

mean= $(\phi_{16}+\phi_{50}+\phi_{84})/3= 0.33$ (COARSE SAND)

Incl. GRAPHIC Std. DEV. O I = $(\phi_{84}-\phi_{16})/4 + (\phi_{95}-\phi_{5})/6.6= 0.73$ (MODERATELY SORTED)

INCL. GRAPHIC SKEWNESS SKI = $((\phi_{16}+\phi_{84}-2\phi_{50})/2(\phi_{84}-\phi_{16})) + ((\phi_{5}+\phi_{95}-2\phi_{50})/2(\phi_{95}-\phi_{5}))= 0.7$

KURTOSIS- KG= $(\phi_{95}-\phi_{5})/2.44(\phi_{75}-\phi_{25})= 0.69$ (PLATYKURTIC)

Table 6: Station 5 Data Table

Station 5						
Mm	µm	Ø	Freq.	Cum Freq.	CF%	Indiv. Pot.
2	2000	-1	1.31	1.31	2.077881	14.37069
1.4	1400	-0.5	1.39	2.7	4.282655	2.20477437
1	1000	0	1.965	4.665	7.399477	3.11682132
0.71	710	0.5	2.865	7.53	11.94385	4.54437307
0.5	500	1	4.545	12.075	19.15299	7.20913633
0.35	350	1.5	9.06	21.135	33.52367	14.3706876
0.25	250	2	15.84	36.975	58.64858	25.1249108
0.18	180	2.5	18.405	55.38	87.84202	29.1934333
0.125	125	3	10.755	66.135	104.9013	17.0592434
0.09	90	3.5	2.55	68.685	108.946	4.04472995

mean= $(\phi_{16}+\phi_{50}+\phi_{84})/3= 1.17$ (COARSE SAND)

Incl. GRAPHIC STD. DEV. O I = $(\phi_{84}-\phi_{16})/4 + (\phi_{95}-\phi_{5})/6.6 = 1.25$ (POORLY SORTED)

INCL. GRAPHIC SKEWNESS SKI = $((\phi_{16}+\phi_{84}-2\phi_{50})/2(\phi_{84}-\phi_{16})) + ((\phi_{5}+\phi_{95}-2\phi_{50})/2(\phi_{95}-\phi_{5}))= -0.59$ (STRONGLY COARSE SKEWED)

KURTOSIS- KG= $(\phi_{95}-\phi_{5})/2.44(\phi_{75}-\phi_{25})= 0.89$ (PLATYKURTIC)

Table 7: Station 6 Data Table

Station 6						
Mm	µm	Ø	Freq.	Cum Freq.	CF%	Indiv. Pot.
2	2000	-1	0.675	0.675	1.070664	14.37069
1.4	1400	-0.5	1.14	1.815	2.878896	1.80823222
1	1000	0	2.03	3.845	6.098818	3.21992228
0.71	710	0.5	3.08	6.925	10.98422	4.88539932
0.5	500	1	3.91	10.835	17.18614	6.20191926
0.35	350	1.5	5.955	16.79	26.63177	9.44563407
0.25	250	2	11.425	28.215	44.75375	18.1219764
0.18	180	2.5	13.075	41.29	65.4929	20.7391546
0.125	125	3	6.335	47.625	75.54128	10.0483781
0.09	90	3.5	1.515	49.14	77.94433	2.40304544

mean= $(\phi_{16}+\phi_{50}+\phi_{84})/3= 1.03$ (COARSE SAND)

Incl. GRAPHIC STD. DEV. O I = $(\phi_{84}-\phi_{16})/4 + (\phi_{95}-\phi_{5})/6.6 = -0.23$ (VERY WELL SORTED)

INCL. GRAPHIC SKEWNESS SKI = $((\phi_{16}+\phi_{84}-2\phi_{50})/2(\phi_{84}-\phi_{16})) + ((\phi_{5}+\phi_{95}-2\phi_{50})/2(\phi_{95}-\phi_{5}))= 20.24$

KURTOSIS- KG= $(\phi_{95}-\phi_{5})/2.44(\phi_{75}-\phi_{25})= 0.027$ (VERY PLATYKURTIC)

Table 8: Station 7 Data Table

Station 7						
Mm	µm	Ø	Freq.	Cum Freq.	CF%	Indiv. Pot.
2	2000	-1	0.27	0.27	0.428266	14.37069
1.4	1400	-0.5	0.665	0.935	1.483068	1.05480213
1	1000	0	2.265	3.2	5.07574	3.5926719
0.71	710	0.5	5.54	8.74	13.86311	8.7873741
0.5	500	1	9.985	18.725	29.70101	15.8378936
0.35	350	1.5	14.48	33.205	52.66873	22.9677215
0.25	250	2	16.555	49.76	78.92775	26.2590213
0.18	180	2.5	13.15	62.91	99.78587	20.8581172
0.125	125	3	5.7	68.61	108.827	9.04116108
0.09	90	3.5	0.95	69.56	110.3339	1.50686018

mean= $(\phi_{16}+\phi_{50}+\phi_{84})/3= 1.72$ (MEDIUM SAND)

Incl. GRAPHIC STD. DEV. O I = $(\phi_{84}-\phi_{16})/4 + (\phi_{95}-\phi_{5})/6.6 = 0.03$ (VERY WELL SORTED)

INCL. GRAPHIC SKEWNESS SKI = $((\phi_{16}+\phi_{84}-2\phi_{50})/2(\phi_{84}-\phi_{16})) + ((\phi_{5}+\phi_{95}-2\phi_{50})/2(\phi_{95}-\phi_{5}))= -0.26$ (STRONGLY COARSE SKEWED)

KURTOSIS- KG= $(\phi_{95}-\phi_{5})/2.44(\phi_{75}-\phi_{25})= 0.86$ (PLATYKURTIC)

Table 9: Station 8 Data Table

Station 8						
Mm	µm	Ø	Freq.	Cum Freq.	CF%	Indiv. Pot.
2	2000	-1	0.07	0.07	0.111032	14.37069
1.4	1400	-0.5	0.22	0.29	0.459989	0.34895709
1	1000	0	0.36	0.65	1.03101	0.5710207
0.71	710	0.5	0.605	1.255	1.990642	0.95963201
0.5	500	1	1.89	3.145	4.9885	2.99785867
0.35	350	1.5	6.81	9.955	15.79031	10.8018082
0.25	250	2	15.63	25.585	40.58212	24.7918154
0.18	180	2.5	22.105	47.69	75.64438	35.0622571
0.125	125	3	15.775	63.465	100.6662	25.0218098
0.09	90	3.5	5.21	68.675	108.9301	8.26393846

mean= $(\phi_{16}+\phi_{50}+\phi_{84})/3= 2.08$ (MEDIUM SAND)

Incl. GRAPHIC STD. DEV. $O I = ((\phi_{84}-\phi_{16})/4 + (\phi_{95}-\phi_{5})/6.6) = 0.5$
(MODERATELY WELL SORTED)

INCL. GRAPHIC SKEWNESS $SKI = ((\phi_{16}+\phi_{84}-2\phi_{50})/2(\phi_{84}-\phi_{16})) + ((\phi_{5}+\phi_{95}-2\phi_{50})/2(\phi_{95}-\phi_{5})) = -0.32$ (STRONGLY COARSE SKEWED)

KURTOSIS- $KG = (\phi_{95}-\phi_{5})/2.44(\phi_{75}-\phi_{25}) = 0.94$ (MESOKURTIC)

Table 10: Station 9 Data Table

Station 9						
Mm	µm	Ø	Freq.	Cum Freq.	CF%	Indiv. Pot.
2	2000	-1	0.31	0.31	0.491712	14.37069
1.4	1400	-0.5	0.84	1.15	1.824094	1.33238163
1	1000	0	1.585	2.735	4.338171	2.51407725
0.71	710	0.5	2.72	5.455	8.65255	4.31437862
0.5	500	1	6.035	11.49	18.22508	9.57252756
0.35	350	1.5	11.535	23.025	36.52153	18.2964549
0.25	250	2	16.145	39.17	62.13022	25.6086922
0.18	180	2.5	16.38	55.55	88.11167	25.9814418
0.125	125	3	10.505	66.055	104.7744	16.6627012
0.09	90	3.5	3.505	69.56	110.3339	5.55952098

mean= $(\phi_{16}+\phi_{50}+\phi_{84})/3= 1.7$ (MEDIUM SAND)

Incl. GRAPHIC STD. DEV. $O I = ((\phi_{84}-\phi_{16})/4 + (\phi_{95}-\phi_{5})/6.6) = 1.9$
(POORLY SORTED)

INCL. GRAPHIC SKEWNESS $SKI = ((\phi_{16}+\phi_{84}-2\phi_{50})/2(\phi_{84}-\phi_{16})) + ((\phi_{5}+\phi_{95}-2\phi_{50})/2(\phi_{95}-\phi_{5})) = -0.28$ (COARSE SKEWED)

KURTOSIS- $KG = (\phi_{95}-\phi_{5})/2.44(\phi_{75}-\phi_{25}) = 1.03$ (MESOKURTIC)

Table 11: Station 10 Data Table

Station10						
Mm	µm	Ø	Freq.	Cum Freq.	CF%	Indiv. Pot.
2	2000	-1	0.305	0.305	0.483781	14.37069
1.4	1400	-0.5	0.885	1.19	1.887541	1.40375922
1	1000	0	1.505	2.695	4.274724	2.38718376
0.71	710	0.5	1.815	4.51	7.15362	2.87889603
0.5	500	1	2.43	6.94	11.00801	3.85438972
0.35	350	1.5	4.335	11.275	17.88405	6.87604092
0.25	250	2	10.76	22.035	34.95123	17.0671742
0.18	180	2.5	19.445	41.48	65.79427	30.8430486
0.125	125	3	18.855	60.335	95.70148	29.9072091
0.09	90	3.5	8.45	68.785	109.1046	13.4031248

mean= $(\phi_{16}+\phi_{50}+\phi_{84})/3= 2.2$ (FINE SAND)

Incl. GRAPHIC STD. DEV. $O I = ((\phi_{84}-\phi_{16})/4 + (\phi_{95}-\phi_{5})/6.6) = 0.78$
(MODERATELY SORTED)

INCL. GRAPHIC SKEWNESS $SKI = ((\phi_{16}+\phi_{84}-2\phi_{50})/2(\phi_{84}-\phi_{16})) + ((\phi_{5}+\phi_{95}-2\phi_{50})/2(\phi_{95}-\phi_{5})) = -0.39$ (STRONGLY COARSE SKEWED)

KURTOSIS- $KG = (\phi_{95}-\phi_{5})/2.44(\phi_{75}-\phi_{25}) = 1.32$ (LEPTOKURTIC)

Table 12: Station 11 Data Table

Station11						
Mm	µm	Ø	Freq.	Cum Freq.	CF%	Indiv. Pot.
2	2000	-1	0.04	0.04	0.063447	14.37069
1.4	1400	-0.5	0.115	0.155	0.245856	0.18240939
1	1000	0	0.29	0.445	0.705845	0.4599889
0.71	710	0.5	0.765	1.21	1.919264	1.21341899
0.5	500	1	1.55	2.76	4.377825	2.45856135
0.35	350	1.5	3.08	5.84	9.263225	4.88539932
0.25	250	2	6.725	12.565	19.93021	10.6669839
0.18	180	2.5	19.16	31.725	50.3212	30.3909906
0.125	125	3	24.745	56.47	89.57094	39.2497422
0.09	90	3.5	11.865	68.335	108.3908	18.8198906

mean= $(\phi_{16}+\phi_{50}+\phi_{84})/3= 2.4$ (FINE SAND)

Incl. GRAPHIC STD. DEV. O I = $(\phi_{84}-\phi_{16})/4 + (\phi_{95}-\phi_{5})/6.6 = 0.51$ (MODERATELY WELL SORTED)

INCL. GRAPHIC SKEWNESS SKI = $((\phi_{16}+\phi_{84}-2\phi_{50})/2(\phi_{84}-\phi_{16})) + ((\phi_{5}+\phi_{95}-2\phi_{50})/2(\phi_{95}-\phi_{5}))= -0.47$ (STRONGLY COARSE SKEWED)

KURTOSIS- KG= $(\phi_{95}-\phi_{5})/2.44(\phi_{75}-\phi_{25})= 1.27$ (LEPTOKURTIC)

Table 13: Station 12 Data Table

Station12						
Mm	µm	Ø	Freq.	Cum Freq.	CF%	Indiv. Pot.
2	2000	-1	0.98	0.98	1.554445	14.37069
1.4	1400	-0.5	2.45	3.43	5.440558	3.88611309
1	1000	0	4.65	8.08	12.81624	7.37568404
0.71	710	0.5	8.275	16.355	25.94179	13.1255452
0.5	500	1	11.83	28.185	44.70616	18.7643747
0.35	350	1.5	13.385	41.57	65.93703	21.2308668
0.25	250	2	12.975	54.545	86.51757	20.5805377
0.18	180	2.5	9.41	63.955	101.4434	14.9258466
0.125	125	3	4.12	68.075	107.9784	6.53501467
0.09	90	3.5	1.45	69.525	110.2784	2.29994448

mean= $(\phi_{16}+\phi_{50}+\phi_{84})/3= 1.08$ (COARSE SAND)

Incl. GRAPHIC STD. DEV. O I = $(\phi_{84}-\phi_{16})/4 + (\phi_{95}-\phi_{5})/6.6 = 0.86$ (MODERATELY SORTED)

INCL. GRAPHIC SKEWNESS KI = $((\phi_{16}+\phi_{84}-2\phi_{50})/2(\phi_{84}-\phi_{16})) + ((\phi_{5}+\phi_{95}-2\phi_{50})/2(\phi_{95}-\phi_{5}))= -0.114$ (COARSE SKEWED)

KURTOSIS- KG= $(\phi_{95}-\phi_{5})/2.44(\phi_{75}-\phi_{25})= 0.90$ (PLATYKURTIC)

Table 14: Station 13 Data Table

Station13						
Mm	µm	Ø	Freq.	Cum Freq.	CF%	Indiv. Pot.
2	2000	-1	5.63	5.63	8.930129	14.37069
1.4	1400	-0.5	3.64	9.27	14.70378	5.77365374
1	1000	0	3.755	13.025	20.65985	5.95606313
0.71	710	0.5	4.86	17.885	28.36863	7.70877944
0.5	500	1	6.34	24.225	38.42493	10.056309
0.35	350	1.5	9.015	33.24	52.72424	14.29931
0.25	250	2	11.77	45.01	71.39345	18.6692045
0.18	180	2.5	12.05	57.06	90.50678	19.1133317
0.125	125	3	6.925	63.985	101.491	10.9842176
0.09	90	3.5	1.725	65.71	104.2271	2.73614085

mean= $(\phi_{16}+\phi_{50}+\phi_{84})/3= 1.13$ (COARSE SAND)

Incl. GRAPHIC STD. DEV. O I = $(\phi_{84}-\phi_{16})/4 + (\phi_{95}-\phi_{5})/6.6 = 1.03$ (POORLY SORTED)

INCL. GRAPHIC SKEWNESS S KI = $((\phi_{16}+\phi_{84}-2\phi_{50})/2(\phi_{84}-\phi_{16})) + ((\phi_{5}+\phi_{95}-2\phi_{50})/2(\phi_{95}-\phi_{5}))= -0.21$ (COARSE SKEWED)

KURTOSIS- KG= $(\phi_{95}-\phi_{5})/2.44(\phi_{75}-\phi_{25})= 0.57$ (VERY PLATYKURTIC)

Table 15 : Station 14 Data Table						
Station14						
Mm	µm	Ø	Freq.	Cum Freq.	CF%	Indiv. Pot.
2	2000	-1	6.875	6.875	10.90491	14.37069
1.4	1400	-0.5	5.76	12.635	20.04124	9.13633119
1	1000	0	4.58	17.215	27.30589	7.26465223
0.71	710	0.5	5.065	22.28	35.33984	8.03394401
0.5	500	1	7.265	29.545	46.86335	11.5235149
0.35	350	1.5	9.16	38.705	61.39266	14.5293045
0.25	250	2	10.445	49.15	77.96019	16.5675311
0.18	180	2.5	9.57	58.72	93.13982	15.1796336
0.125	125	3	5.49	64.21	101.8479	8.70806567
0.09	90	3.5	1.615	65.825	104.4095	2.5616623

mean= $(\phi_{16} + \phi_{50} + \phi_{84}) / 3 = 2.65$ (FINE SAND)

Incl. GRAPHIC STd. DEV. $O I = ((\phi_{84} - \phi_{16}) / 4 + (\phi_{95} - \phi_{5}) / 6.6) = 1.1$ (POORLY SORTED)

INCL SKI = $((\phi_{16} + \phi_{84} - 2\phi_{50}) / 2(\phi_{84} - \phi_{16})) + ((\phi_{5} + \phi_{95} - 2\phi_{50}) / 2(\phi_{95} - \phi_{5})) = 0.18$ (FINE SKEWED)

KURTOSIS- KG= $(\phi_{95} - \phi_{5}) / 2.44(\phi_{75} - \phi_{25}) = 0.50$ (VERY PLATYKURTI

Table 16: Grain Size Scales for Sediments			
Mean size	Skewness	Kurtosis	Inclusive Graphic Standard deviation (ϕ_i^ϕ)
0.00 0.25 0.50 0.75 1.00 COARSE SAND	-1.0 to +0.30 strongly fine skewed	< 0.7 very platykurtic	< 0.35 very well sorted
1.25 1.50 1.75 2.00 MEDIUM SAND			0.35 – 0.5 well sorted
2.25 2.50 2.75 3.00 FINE SAND	+0.3 to +0.10 fine skewed	0.67 – 0.90 platykurtic	0.5 – 0.71 moderately well sorted
3.25 3.50 3.75 4.00 VERY FINE SAND	+0.1 to -0.10 near symmetrical	0.90 to 1.11 Mesokurtic	0.71 – 1.0 moderately sorted
	-0.1 to -0.30 coarse skewed	1.11 to 1.50 Leptokurtic	1.0 – 2.0 poorly sorted
	-0.3 to -1.00 strongly coarse skewed	1.5 to 3.00 very leptokurtic	2.0 – 4.0 very poorly sorted
		> 3.0 Extremely Leptokurtic	> 4.0 Extremely poorly sorted

4. CONCLUSION

This study successfully integrates Acoustic Doppler Current Profiler (ADCP) data with grain size analysis to elucidate sediment deposition dynamics within a lagoonal environment. The findings indicate a clear relationship between sediment velocity and grain size distribution, with high sediment velocities associated with coarser grains, while lower velocities correlate with finer sediments. The identified high velocity zones at depths of 21 to 27 ft and 12 to 19 ft provide critical insights for optimizing marine navigation routes, suggesting that vessels should favor these areas to enhance safety and efficiency. The analysis also highlights the necessity of strategic dredging along the lagoon's edges to mitigate sediment accumulation, which poses challenges to marine transport and aquatic ecosystems. This approach not only facilitates smoother navigation but also contributes to sustainable sediment management practices. Moreover, the results emphasize the importance of continuous monitoring of sediment dynamics using ADCP technology, which can inform coastal engineering projects and enhance our understanding of sediment transport processes. By providing a comprehensive overview of sediment movement and deposition patterns, this study lays the groundwork for future research aimed at improving marine transportation safety and ecosystem health. In summary, the integration of ADCP data with grain size analysis offers valuable insights for stakeholders involved in marine transport, environmental management, and coastal

engineering, underscoring the need for ongoing research in sediment dynamics to inform effective decision-making and policy development.

RECOMMENDATION

Optimal Navigation Routes: Marine transport operators should prioritize navigation through the identified high velocity zones at depths of 21 to 27 ft and 12 to 19 ft. Regular updates and dissemination of navigational charts that highlight these routes will enhance safety and efficiency for vessels operating in the lagoon.

Dredging Operations: To mitigate sediment accumulation, it is recommended that dredging activities be conducted along the lagoon's edges, particularly in areas identified with low velocities. This approach will not only facilitate improved navigation but also help maintain the ecological balance within the lagoon.

Monitoring and Maintenance: Establish a regular monitoring program utilizing ADCP technology to track sediment deposition and water velocity changes over time. This will provide valuable data for ongoing sediment management and help anticipate shifts in sediment dynamics that could affect marine transport and ecosystems.

Further Research: Additional studies could be conducted to explore the

seasonal and temporal variations in sediment deposition and transport. Understanding how these factors interact will enhance predictive models and inform more effective management strategies.

REFERENCES

- Edokpayi, C.A., and Ikharo, E.A., 2010. The Malaco-Faunal Characteristics of the 'Sandwiched' Epe Lagoon, Lagos. Science publications, Pp. 10-11.
- Fondriest Environmental, Inc. 2014. Sediment Transport and Deposition. Retrieved June 10, 2021, from Fundamentals of Environmental Measurements.: <https://www.fondriest.com/environmental-measurements/parameters/hydrology/sediment-transport-depositi>
- Kusemiju, K., 1988. Strategies for effective management of water hyacinth in the creeks and lagoons of south-western Nigeria. In: Oke, K.L.; A.M.A. Imevbore and T.A. Farri, Op.cit., Pp. 39-45.
- Osuagwu., J.C. Nwachukwu, A.N. Nwoke, H.U., Agbo, K.C., 2014. Effects of Soil Erosion and Sediment Deposition on Surface Water Quality: A Case Study of Otamiri River. Asian Journal of Engineering and Technology Volume 02 – Issue 05, October 2014
- Sherman, D.J., Davis, L., and Namikas, S.L., 2013. Sediments and Sediment Transport. In: John F. Shroder (ed.) Treatise on Geomorphology, 1, Pp. 233-256. San Diego: Academic Press.
- Woods., 2021. Hole Oceanographic Institution.,2017, April 12. Acoustic Doppler Current Profiler (ADCP). Retrieved from WHO <https://www.whoi.edu/what-we-do/explore/instruments/instruments-sensors-samplers/acoustic-doppler-current-profiler-adcp/>

